JPE 16-6-34

http://dx.doi.org/10.6113/JPE.2016.16.6.2350
ISSN(Print): 1598-2092 / ISSN(Online): 2093-4718

An Improved One Cycle Control for Active Power Filters under Non-Ideal Voltage Conditions

Lei Wang[*,**], Chunguang Ren[*,**], Yu Yang[***], Xiaoqing Han[†,**], and Peng Wang[****]

[*,†]College of Electrical and Power Engineering, Taiyuan University of Technology, Taiyuan, China
[**]Shanxi Key Lab of Power System Operation and Control, Taiyuan University of Technology, Taiyuan, China
[***]Shanxi Electric Power Corporation, Taiyuan, China
[****]Nanyang Technological University, Jurong West, Singapore

Abstract

The one cycle control (OCC) scheme for active power filters (APFs) has shown excellent harmonic suppression and implementation simplicity. However, its real world application is limited because the non-ideal supply voltage for APFs can influence its performance so that the source currents are still distorted after compensation. This paper proposes a modified one cycle control (MOCC) scheme to improve the performance of three-phase shunt APFs under non-ideal supply voltage conditions. In this paper a detailed mathematical derivation has been presented and the key control law of the MOCC has been developed for adaption to the non-ideal supply voltages, following the control philosophy of simplicity. A relatively simple sequence filter is introduced to extract the harmonic components of supply voltages. The modified scheme can be easily implemented. The proposed control strategy has excellent performance and a 5kVA APF hardware platform has been implemented to validate the feasibility and performance of the proposed strategy.

Key words: Active Power Filters (APFs), Non-ideal voltage, One Cycle Control (OCC)

I. INTRODUCTION

The rapid increase in nonlinear loads has resulted in a lot of harmonic currents. These harmonic currents can lead to instability, voltage distortion and interference with electronic appliances. The active power filter (APF) is a viable solution for these problems [1]-[3]. APFs are connected in parallel with nonlinear loads and act as a controlled current source to compensate the harmonic and reactive currents.

The Synchronous Reference Frame (SRF) and the Instantaneous Reactive Power Theory (IRPT) are two typical methods employed in APFs. In the SRF [4]-[9], through Park transformations the load currents are transformed from the *a-b-c* frame into the *d-q-o* frame to generate compensation reference currents. However, this method requires a Phase Locking Loop (PLL) to act as a reference for calculating harmonic quantity. The presence of the PLL increases the computational complexity and reduces the robustness of the controller. Especially, an unbalanced and distorted supply voltage leads to more difficulties for the implementation of a PLL. In the IRPT [10]-[15], instantaneous harmonic power is calculated to obtain compensation reference currents. Although this method does not need a PLL, it requires a complicated control structure for implementation. In addition, under non-ideal supply voltage conditions, the performance of an IRPT-based APF is not satisfactory because distorted supply voltages influence the accuracy of the instantaneous powers and compensation reference currents. The above two methods need specially designed current controllers with a high bandwidth to generate compensation currents. Although hysteresis control [16] has a broad current-loop bandwidth, the performance of this controller suffers due to its variable switching frequency.

A simple One Cycle Control (OCC) has been applied to APFs [17]-[23]. This OCC-based APF can be implemented without a PLL. Its control structure is simple and it does not

Manuscript received Apr. 22, 2016; accepted Aug. 27, 2016
Recommended for publication by Associate Editor Kyo-Beum Lee.
[†]Corresponding Author: hanxiaoqing@tyut.edu.cn
Tel: +86-0351-1760, Taiyuan University of Technology
[*]College of Electrical and Power Engineering, Taiyuan University of Technology, China
[**]Shanxi Key Lab of Power System Operation and Control, Taiyuan University of Technology, China
[***]Shanxi Electric Power Corporation, China
[****]Nanyang Technological University, Singapore

require complicated algorithms, and can be realized by analog devices. Meanwhile the OCC scheme operates with a constant switching frequency and has a high bandwidth owing to the nonlinear feature of its current controller. In spite of the above superiorities, the application of OCC is limited and its performance deteriorates seriously under non-ideal supply voltage conditions. The authors of [18] proposed an OCC scheme for three-phase bipolar mode active power filters. They also demonstrated a defect through simulation results since its three-phase currents are unbalanced under unbalanced voltage conditions. Ref. [23] analyzed the theoretical operation characteristic of an OCC-based APF under unbalanced voltage conditions. However, the aforementioned references did not propose a solution for this problem. The authors of [24] proposed an OCC strategy that can work in the case of an unbalanced grid voltage. However, it only takes into consideration unbalanced voltage caused by common mode voltage. It is not a viable solution for APFs under general non-ideal voltage conditions.

This paper proposes a Modified OCC (MOCC) to improve the performance of three-phase APFs under non-ideal supply voltage conditions. The control core of the MOCC is presented through detailed analytical studies and mathematical derivation. This control strategy can guarantee excellent performance in terms of compensating harmonics and it overcomes the defects of the conventional OCC i.e. the source currents are easily affected by the distorted supply voltages. The modified scheme is easy to implement. A simple extension rather than a complex control algorithm is embedded within the original OCC. The feasibility and performance of the MOCC has been validated by experimental studies on a 5 kVA APF hardware platform developed in the laboratory.

II. Operation of an OCC-based APF

Fig. 1 shows a schematic of a three-phase shunt APF with nonlinear loads at the point of common coupling (PCC), where (v_a, v_b, v_c) are the three-phase supply voltages, L and C_{dc} represent the inductance and capacitance, respectively, v_{dc} is the capacitor voltage on the dc side, (i_a, i_b, i_c), (i_{la}, i_{lb}, i_{lc}) and (i_{fa}, i_{fb}, i_{fc}) are the three-phase currents on the source, load and filter sides, respectively, and (S_{ap}, S_{bp}, S_{cp}) and (S_{an}, S_{bn}, S_{cn}) are the upper and lower switches of the three limbs, respectively. The OCC control block generates drive pulses for the switches. In order to demonstrate the MOCC, an existing control strategy is briefly represented, which was described in [17]. The control goal of the OCC is to guarantee the loads with an APF as a linear resistive load from the viewpoint of the ac supply side, which meets the following relationship:

$$R_s i_x = v_m - 2v_m d_x, \qquad x = a,b,c \tag{1}$$

where d_x is the duty ratio for the switches, R_s represents the gain of the current sensors, and v_m is the reference signal, which contains information on the load active current.

In each switching cycle, if d_x is controlled to satisfy (1), the source currents are regulated to be sine in shape, and the reactive and harmonic components are eliminated. The control block of the OCC, shown in the shaded part of Fig. 2, adopts a dual-loop control structure. v_{dc} is sensed and the error between v_{dc} and v_{dcref} is fed to a simple PI controller. v_m is obtained from the output of the PI controller. Then v_m is processed by an integrator and summed with the output of the integrator. When the integral quantity reaches $R_s i_x$, the flip-flops which are set at the beginning of every clock are reset. The outputs of the flip-flops are drive pulses for the switches. The control law (1) can be realized through simple circuits, and the above control process is repeated in every switching cycle that is decided by the clock.

III. The MOCC Scheme

Under unbalanced and distorted supply voltage conditions, a three-phase converter cannot be simplified as three identical and independent single-phase systems, and (1) is not applied to APFs. Therefore, the operation of the OCC-based APF must be influenced and an improved OCC is developed.

Non-ideal three-phase voltages can be broken down into positive sequence, negative sequence and zero sequence components at different frequencies. This can be expressed as:

$$\begin{cases} v_a = \sum_{h=1}^{\infty}\left(v_{ah}^{+} + v_{ah}^{-} + v_{ah}^{0}\right) \\ v_b = \sum_{h=1}^{\infty}\left(v_{bh}^{+} + v_{bh}^{-} + v_{bh}^{0}\right) \\ v_c = \sum_{h=1}^{\infty}\left(v_{ch}^{+} + v_{ch}^{-} + v_{ch}^{0}\right) \end{cases} \tag{2}$$

where the subscript h represents the harmonic order of the voltage, the superscripts '+', '-' and '0' denote the positive sequence, negative sequence and zero sequence components, respectively. The sum of the three-phase voltages is as follows:

$$\begin{aligned} \frac{1}{3}\left(v_a + v_b + v_c\right) &= \frac{1}{3}\sum_{h=1}^{\infty}\left(v_{ah}^{0} + v_{bh}^{0} + v_{ch}^{0}\right) \\ &= \sum_{h=1}^{\infty} v_{ah}^{0} = \sum_{h=1}^{\infty} v_{bh}^{0} = \sum_{h=1}^{\infty} v_{ch}^{0} = v_0 \end{aligned} \tag{3}$$

where v_0 represents the zero sequence voltage.

Since the filter inductances L are small, the voltages across the inductors can be neglected [18]. Hence, the supply voltages can be approximated as follows:

$$\begin{cases} v_a \approx v_{AO} = v_{AN} + v_{NO} \\ v_b \approx v_{BO} = v_{BN} + v_{NO} \\ v_c \approx v_{CO} = v_{CN} + v_{NO} \end{cases} \tag{4}$$

where (v_{AO}, v_{BO}, v_{CO}) and (v_{AN}, v_{BN}, v_{CN}) represent the average

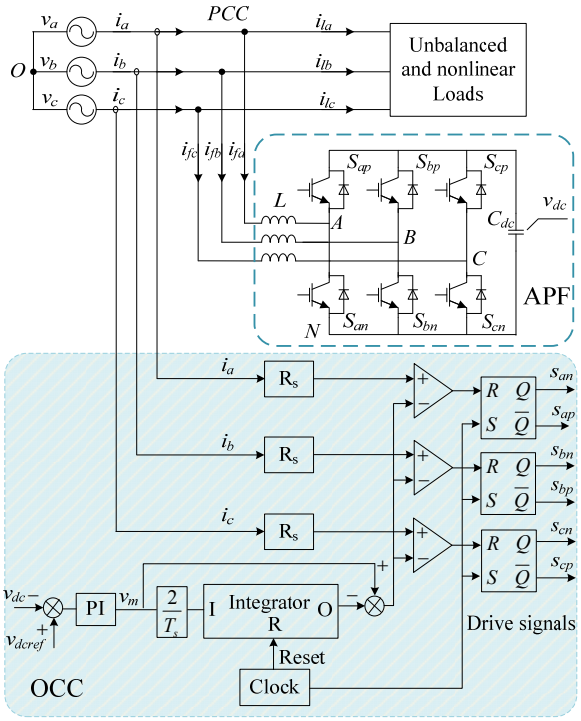

Fig. 1. Schematic of the three-phase shunt APF with the existing OCC.

voltages at the nodes A, B, and C referred to the neutral 'O' and the node 'N' respectively. In addition, v_{NO} represents the average voltage at the node 'N' referred to the neutral 'O'. Combining (3) with (4), yields:

$$v_{NO} \approx v_0 - \frac{1}{3}\left(v_{AN} + v_{BN} + v_{CN}\right) \tag{5}$$

By substituting (5) into (4), the relationship between (v_a, v_b, v_c) and (v_{AN}, v_{BN}, v_{CN}) can be obtained as:

$$\begin{cases} v_a \approx v_{AN} - \frac{1}{3}\left(v_{AN} + v_{BN} + v_{CN}\right) + v_0 \\ v_b \approx v_{BN} - \frac{1}{3}\left(v_{AN} + v_{BN} + v_{CN}\right) + v_0 \\ v_c \approx v_{CN} - \frac{1}{3}\left(v_{AN} + v_{BN} + v_{CN}\right) + v_0 \end{cases} \tag{6}$$

The equations for (v_{AN}, v_{BN}, v_{CN}) and (d_{an}, d_{bn}, d_{cn}) [18] are:

$$\begin{cases} v_{AN} = \left(1 - d_{an}\right) v_{dc} \\ v_{BN} = \left(1 - d_{bn}\right) v_{dc} \\ v_{CN} = \left(1 - d_{cn}\right) v_{dc} \end{cases} \tag{7}$$

Therefore, combining (6), (7) and (2), the relationships between the supply voltage and the duty ratio are derived as follows:

$$\begin{bmatrix} -\frac{2}{3} & \frac{1}{3} & \frac{1}{3} \\ \frac{1}{3} & -\frac{2}{3} & \frac{1}{3} \\ \frac{1}{3} & \frac{1}{3} & -\frac{2}{3} \end{bmatrix} \begin{bmatrix} d_{an} \\ d_{bn} \\ d_{cn} \end{bmatrix} = \frac{1}{v_{dc}} \begin{bmatrix} \sum_{h=1}^{\infty}\left(v_{ah}^{+} + v_{ah}^{-}\right) \\ \sum_{h=1}^{\infty}\left(v_{bh}^{+} + v_{bh}^{-}\right) \\ \sum_{h=1}^{\infty}\left(v_{ch}^{+} + v_{ch}^{-}\right) \end{bmatrix} \tag{8}$$

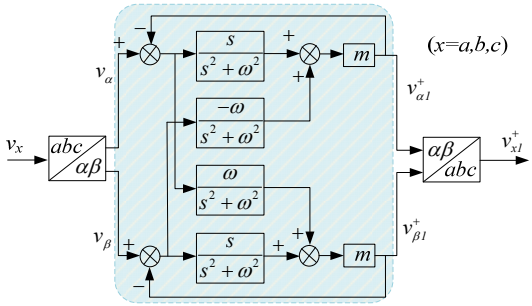

Fig. 2. The block diagram of the extracting method based on the FPSF.

Since the matrix in (8) is singular, it has no unique solution. One possible solution is:

$$\begin{cases} d_{an} = k - \frac{1}{v_{dc}} \sum_{h=1}^{\infty}\left(v_{ah}^{+} + v_{ah}^{-}\right) \\ d_{bn} = k - \frac{1}{v_{dc}} \sum_{h=1}^{\infty}\left(v_{bh}^{+} + v_{bh}^{-}\right) \\ d_{cn} = k - \frac{1}{v_{dc}} \sum_{h=1}^{\infty}\left(v_{ch}^{+} + v_{ch}^{-}\right) \end{cases} \tag{9}$$

where k is a variable, and the value of k is determined based on the control equation of the OCC. Hence, according to the control equation in [17][18][20], the value of k can be determined as 0.5. Let k=0.5, then equation (9) becomes:

$$\begin{cases} \left(1 - 2d_{an}\right) = \frac{2}{v_{dc}} \sum_{h=1}^{\infty}\left(v_{ah}^{+} + v_{ah}^{-}\right) \\ \left(1 - 2d_{bn}\right) = \frac{2}{v_{dc}} \sum_{h=1}^{\infty}\left(v_{bh}^{+} + v_{bh}^{-}\right) \\ \left(1 - 2d_{cn}\right) = \frac{2}{v_{dc}} \sum_{h=1}^{\infty}\left(v_{ch}^{+} + v_{ch}^{-}\right) \end{cases} \tag{10}$$

By substituting (10) into (1), the source currents can be expressed as follows:

$$\begin{aligned} i_x &= \frac{v_m}{R_s}\left(1 - 2d_x\right) \\ &= \frac{2v_m}{R_s v_{dc}} \sum_{h=1}^{\infty}\left(v_{xh}^{+} + v_{xh}^{-}\right), \quad x = a,b,c \end{aligned} \tag{11}$$

It can be inferred from (11) that if the OCC follows the control law (1) under non-ideal voltage conditions, the source currents will still be distorted after compensation. They will be proportional to the sum of the positive sequence and negative sequence voltages at all frequencies.

For a deeper analysis, the source currents are also divided into positive sequence and negative sequence components at different frequencies. (11) can be rewritten as:

$$\sum_{h=1}^{\infty}\left(i_{xh}^{+} + i_{xh}^{-}\right) = \frac{2v_m}{R_s v_{dc}} \sum_{h=1}^{\infty}\left(v_{xh}^{+} + v_{xh}^{-}\right) \tag{12}$$

Since $(2v_m)/(R_s v_{dc})$ is a linear scale factor, it can be treated as a virtual linear conductance. Therefore, the fundamental positive sequence current i_{x1}^{+} is proportional to the

fundamental positive sequence voltage v_{x1}^{+} and the rest of the currents that are undesired components are proportional to the rest of the combined voltage. The undesired components of the currents can be expressed as follows:

$$i_{x1}^{-}+\sum_{h=2}^{\infty}\left(i_{xh}^{+}+i_{xh}^{-}\right)=\frac{2v_m}{R_s v_{dc}}\left(v_{x1}^{-}+\sum_{h=2}^{\infty}\left(v_{xh}^{+}+v_{xh}^{-}\right)\right) \quad (13)$$

By substituting (13) into (1), the control law of the OCC is modified as follows:

$$\begin{aligned} v_m-2v_m d_x &= R_s\left(i_{xf}^{+}+i_{x1}^{-}+\sum_{h=2}^{\infty}\left(i_{xh}^{+}+i_{xh}^{-}\right)\right) \\ &= R_s i_{xf}^{+}+\frac{2v_m}{v_{dc}}\left(v_{x1}^{-}+\sum_{h=2}^{\infty}\left(v_{xh}^{+}+v_{xh}^{-}\right)\right) \\ &= R_s i_{xf}^{+}+\frac{2v_m}{v_{dc}}\left(v_x-v_{x1}^{+}-v_0\right) \end{aligned} \quad (14)$$

In (14) v_{x1}^{+} and v_0 are introduced into the control law of the OCC, and the source currents as objective of the OCC scheme only include i_{x1}^{+}. Therefore, if the fundamental positive sequence voltages and zero sequence voltage can be obtained and scaled by $(2v_m)/v_{dc}$ to form the control law (14), the source currents after compensation can be kept balanced and sinusoidal even under unbalanced and distorted supply voltage conditions.

For the realization of the MOCC, (14) also needs the fundamental positive sequence and zero sequence components of the supply voltages to implement this control scheme compared with (1). The zero sequence voltage can be obtained easily by the sum of the three-phase supply voltages as in (3). Hence, a method for extracting the fundamental positive sequence voltage is critical for the MOCC. A common extraction method is the aforementioned SRF method. However the SRF method, which is complex due to the requirement of the PLL, is contradictory to the control philosophy of the OCC's simplicity and improper for the MOCC. In order to address this problem, a relatively simple extraction method is employed.

Fig. 2 shows the structure of the proposed extraction method. In Fig. 2 the shaded part is the fundamental positive sequence filter (FPSF), (v_α, v_β) and ($v_{\alpha 1}^{+}$, $v_{\beta 1}^{+}$) are the supply voltages and fundamental positive sequence supply voltages in the α-β frame, respectively, ω is the angular synchronous speed with the fundamental frequency, and m is a constant which controls the bandwidth and the response speed of the FPSF [25]. Three-phase voltages, as shown in Fig. 2, are measured and transformed into the α-β frame. Then they are fed into the FPSF. Through the given filter, the signals of the fundamental negative sequence and other frequencies are reduced to be negligible and only the fundamental positive sequence component is obtained from the output of the FPSF.

The parameter m can significantly influence the performance of the FPSF. In a positive sequence system, the voltage in the α axis leads the voltage in the β axis by 90 degrees. The FPSF in the shaded part of Fig. 2 can be equivalent to the system shown in Fig. 3, where ω/s represents the transfer function of a 90 degrees phase shift. The close loop transfer function of the FPSF can be derived as follows:

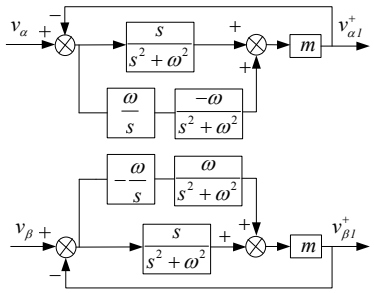

Fig. 3. The equivalent block diagram of the FPSF.

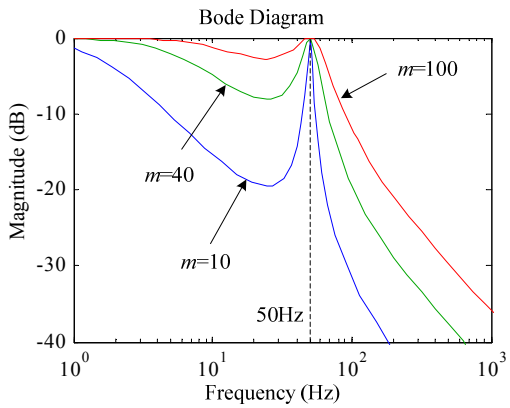

Fig. 4. The Bode diagram of the FPSF as the m changes.

$$C_f(s)=\frac{ms^2-m\omega^2}{s^3+ms^2+s\omega^2-m\omega^2} \quad (15)$$

Fig. 4 shows a bode diagram of the FPSF with the change of m. It can be seen that the band pass frequency of the FPSF is 50Hz regardless of the value of m. This guarantees the excellent steady-state performance of extracting the fundamental component of the voltage. Meanwhile, the bandwidth of the FPSF varies with the value of m, which influences the transient performance of the FPSF. As m increases, the bandwidth becomes broader and the response becomes faster. However, an increased m may worsen the performance of the filter. Therefore, m should be chosen in a proper range.

Finally, the MOCC can be implemented relatively simply and with less computation to guarantee the sine shape and unity power factor of the source currents under unbalanced and distorted supply voltage conditions. The control law of the MOCC is depicted in detail in Fig. 5.

IV. Simulated and Experimental Results

In order to demonstrate the performance of a MOCC-based three-phase shunt APF, firstly, detailed simulation studies are

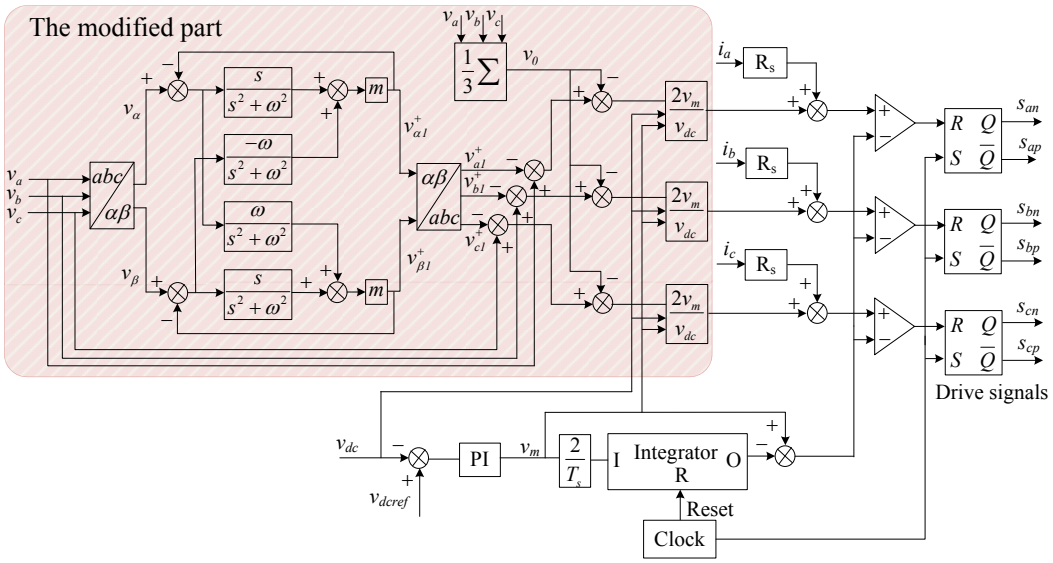

Fig. 5. The control block diagram of the MOCC.

TABLE I
SIMULATION AND EXPERIMENT PARAMETERS

Parameters	Simulation	Experiment
Supply voltage	220V	50V
Frequency	50Hz	50Hz
Dc voltage	800V	180V
Inductor	1mH	3mH
DC side capacitor	3300uF	3300uF
Switching frequency	25kHz	12.8kHz
m	40	40
Voltage loop PI	k_p=0.4, k_i=8	k_p=0.4, k_i=4
Unbalanced loads	15Ω/20Ω/20Ω	
Rectifier load	3mH, 20Ω	

carried out in Matlab/Simulink using the PLECS libraries. The system parameters in the simulation studies are provided in Table I. The loads are composed of three-phase unbalanced loads and a full bridge rectifier with resistors in the dc side.

The proposed control strategy is compared with a common SRF method and the conventional OCC scheme. The simulation results are demonstrated with the combined voltages where an additional 10% voltage is added to the phase-A voltage and a 10% fifth harmonic voltage is added to the three-phase supply voltages. Fig. 6(a) shows the combined non-ideal supply voltages. Fig. 6(b) shows the three-phase source currents with unbalanced and nonlinear loads before compensation. Fig. 7(a) shows steady-state waveforms of the three-phase source currents with a common SRF method that adopts a single synchronous reference frame software PLL (SSRF-SPLL). It can be seen from Fig. 7(a) that the source currents are distorted under non-ideal voltage conditions because the SSRF-SPLL in the SRF method is significantly influenced by the distorted voltages. Fig. 7(b) shows the three-phase source currents that employed the

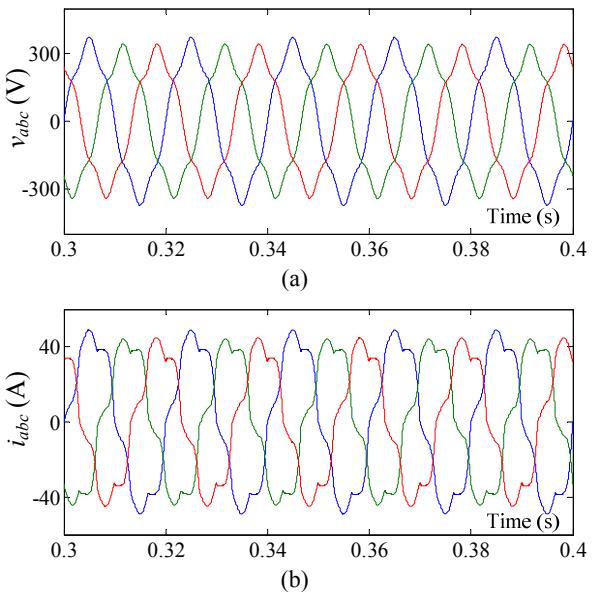

Fig. 6. The simulated waveforms of the supply voltages and source currents before compensation. (a) Three-phase unbalanced and distorted supply voltages. (b) Three-phase source currents.

OCC after compensation. It is evident that (i_a, i_b, i_c) are unbalanced and distorted heavily. Fig. 7(c) shows the performance of the MOCC under the same conditions. By contrast, (i_a, i_b, i_c) are regulated to be sine shape and balanced. The performance of the MOCC-based APF is significantly improved. Fig. 8 shows detailed waveforms of the phase-A voltage, source current, load current and compensation current. Moreover, the frequency spectrums of the phase-A voltage and source current with two different methods are shown in Fig. 9. It can be seen that i_a with the OCC after compensation in Fig. 9(c) contains amounts of the 3rd harmonic and that it has almost the same order of harmonic

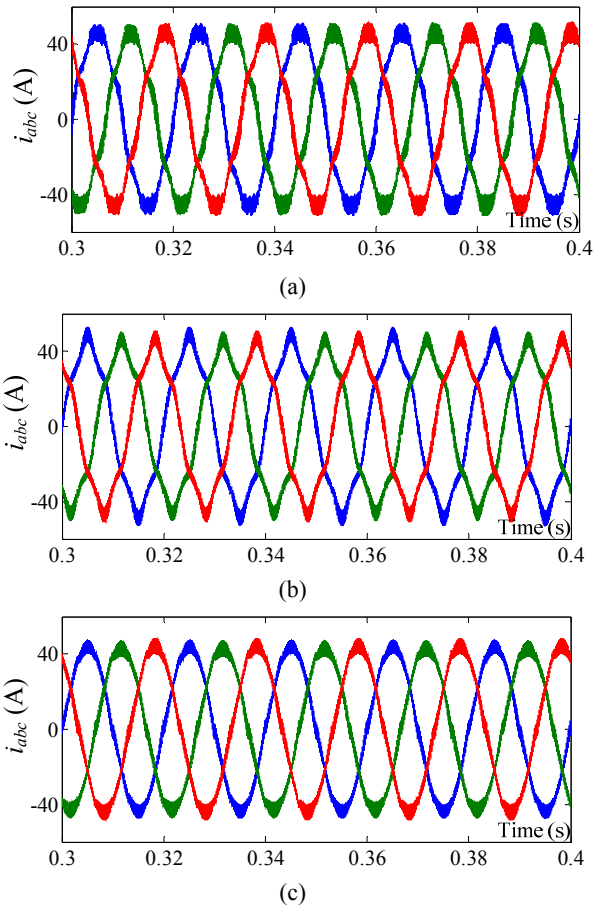

Fig. 7. The simulated waveforms of the source currents with two different methods after compensation. (a) The source currents with the common SRF method. (b) The source currents with the OCC. (c) The source currents with the MOCC.

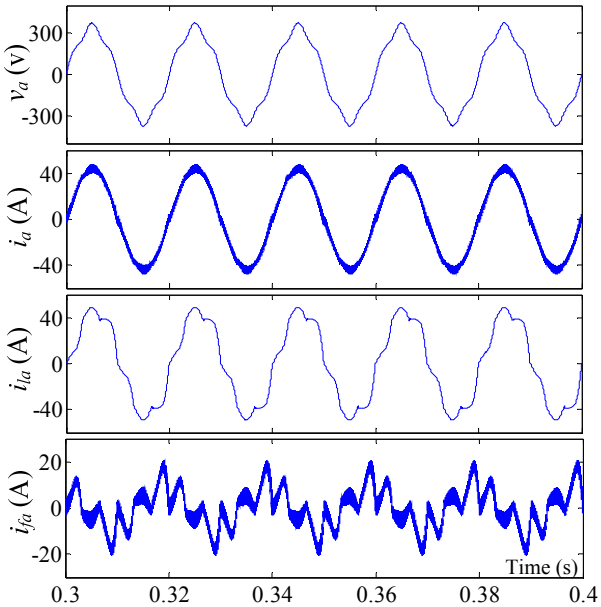

Fig. 8. The simulated waveforms of the phase-A voltage and current at the source, load and filter sides respectively with the MOCC after compensation.

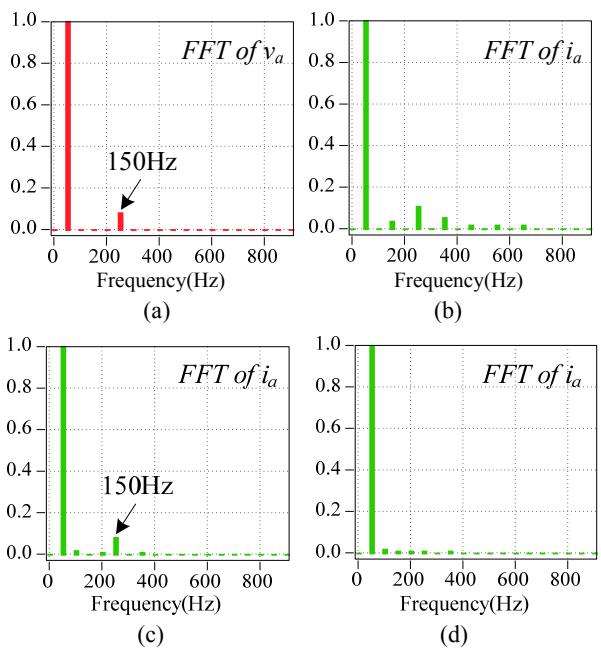

Fig. 9. The simulated results of the frequency spectrum of the voltage and current with two different methods. (a) The phase-A voltage. (b) The phase-A source current before compensation. (c) The phase-A source current with the OCC. (d) The phase-A source current with the MOCC.

as the supply voltage. Meanwhile, the harmonic components of i_a with the MOCC in Fig. 9(d) are almost negligible. As shown in Figs. 6-9, the MOCC can address the aforementioned problems well and presents better performance under non-ideal supply voltage conditions.

An experimental platform, shown in Fig. 10, has been developed to verify the performance of the MOCC scheme. The MOCC is implemented on a DSP. The source current signals are provided by LT 108-S7/sp1 Hall Effect current sensors and the voltage signals are provided by LV 25-P LEM voltage sensors. A Concept 2SC0108T is applied to drive the IGBTs. The switching frequency is 12.8 kHz. An RC filter with a 2 kHz cut-off frequency is connected at the Point of Common Coupling (PCC) for suppressing the switching harmonics. The load is a programmable RCD nonlinear load which is composed of resistors, capacitors and diode rectifiers. The ac power supply is an autotransformer. The experiment parameters are shown in Table I. The controller gains are tuned by a HMI.

Fig. 11(a) shows the supply voltages which are unbalanced (63v, 50v, 52v) and contain a small quantity of 3rd harmonic. Fig. 11(b) shows the source currents with unbalanced and nonlinear loads before compensation. Fig. 12 presents the performance of an APF with two different OCC schemes. Fig. 12(a) shows the source currents with the existing OCC after compensation. (i_a, i_b, i_c) are regulated to be sine shape. However, they are still heavily unbalanced. The currents are 1.27A, 1.05A and 1.1A. Fig. 12(b) shows the performance of the MOCC. It can be seen that the source currents are

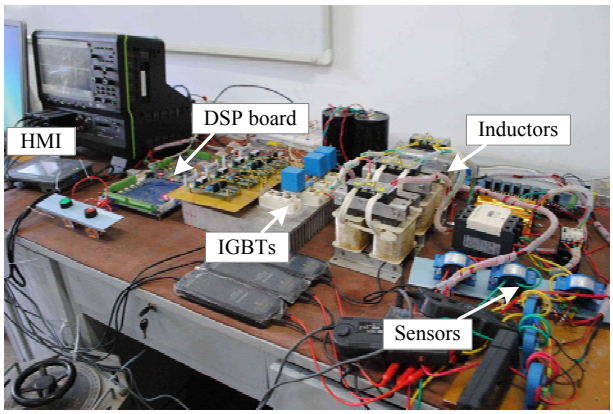

Fig. 10. The hardware platform of the proposed system.

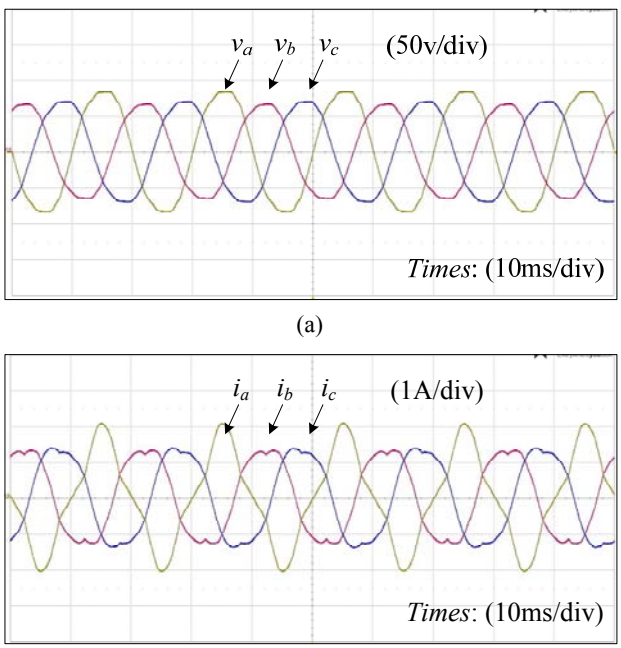

Fig. 11. The experimental waveforms of supply voltage and current before compensation. (a) Three-phase supply voltages. (b) Three-phase source currents.

significantly improved and that they are almost sinusoidal and balanced. These currents are 1.15A, 1.19A and 1.16A. Fig. 13 presents the frequency spectrums of the phase-A voltage and source current. They are obtained by the frequency spectrum analyzer embedded in the oscilloscope. i_a with the OCC in Fig. 13(c) has almost the same order harmonic component as the supply voltage in Fig. 13(a) after compensation, including the 3rd harmonic. By comparing Fig. 13(c) and Fig. 13(d), the performance of the MOCC-based APF is considerably improved. It can be seen from the experimental results in Figs. 11-13 that the MOCC scheme is able to address the problems where the source currents after compensation are easily affected by non-ideal supply voltages and can guarantee the excellent performance of the APFs.

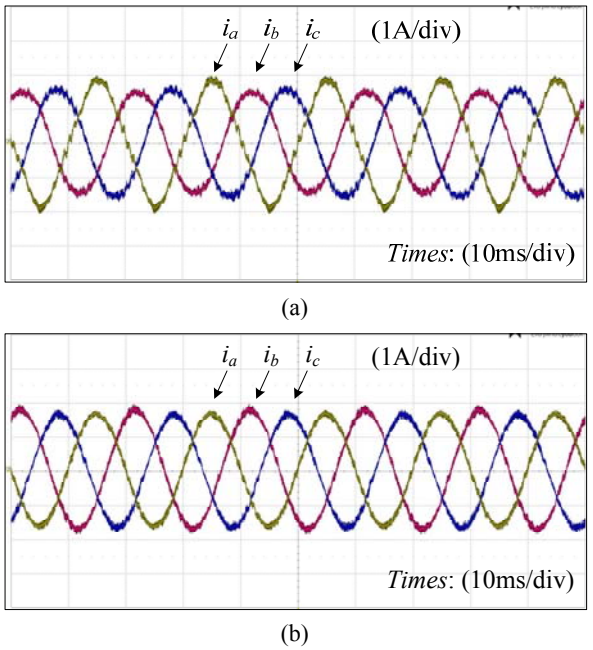

Fig. 12. The experimental waveforms of the source currents with two different methods after compensation. (a) The source currents with the OCC. (b) The source currents with the MOCC.

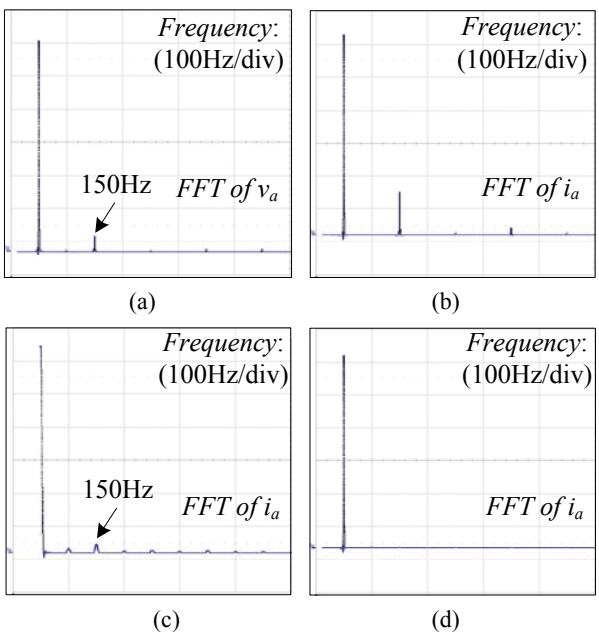

Fig. 13. The experimental results of the frequency spectrum of the voltage and current with two different methods. (a) The phase-A voltage. (b) The phase-A source current before compensation. (c) The phase-A source current with the OCC. (d) The phase-A source current with the MOCC.

V. CONCLUSIONS

OCC schemes are widely used in various convertors due to their simplicity. However, the application of OCC-based APFs is limited because real world non-ideal supply voltage can influence the compensation precision of the APF. This paper proposed a MOCC scheme to improve the performance

of APFs under non-ideal voltage conditions. In this paper, the operation of an existing OCC-based APF has been studied, and the control core of the MOCC is presented through detailed analytical studies and mathematical derivations. A 5kVA APF hardware platform has been set up and the experimental results show that the MOCC significantly improves the performance in terms of compensation when compared with the conventional OCC in a non-ideal network. The proposed method effectively deals with the issues where source currents after compensation are easily affected by non-ideal supply voltages. Furthermore, the MOCC maintains the control philosophy of simplicity and has the advantages of the existing OCC.

ACKNOWLEDGMENT

Financial Supports from Shanxi key projects of coal based science and technology (MD2014-06), and Shanxi Province Scientific Research Foundation for Returned Scholars (2015-Key Project 1) are gratefully acknowledged.

REFERENCES

[1] H. Akagi, "New trends in active filters for power conditioning," *IEEE Trans. Ind. Appl.*, Vol. 32, No. 2, pp. 1312-1332, Nov./Dec. 1996.

[2] B. Singh, K. Al-Haddad, and A. Chandra, "A review of active filters for power quality improvement," *IEEE Trans. Ind. Electron.*, Vol. 46, No. 5, pp. 960-971, Oct. 1999.

[3] L. Asiminoaei, F. Blaabjerg, and S. Hansen, "Detection is key—Harmonic detection methods for active power filter applications," *IEEE Ind. Appl. Mag.*, Vol. 13, No. 4, pp. 22-33, Jul./Aug. 2007.

[4] M. J. Newman, D. N. Zmood, and D. G. Holmes, "Stationary frame harmonic reference generation for active filter systems," *IEEE Trans. Ind. Appl*., Vol. 38, No. 6, pp. 1591-1599, Nov./Dec. 2002.

[5] C. Lascu, L. Asiminoaei, I. Boldea, and F. Blaabjerg, "High performance current controller for selective harmonic compensation in active power filters," *IEEE Trans. Power Electron.*, Vol. 22, No. 5, pp. 1826-1835, Sep. 2007.

[6] M. Kesler and E. Ozdemir, "Synchronous reference frame based control method for UPQC under unbalanced and distorted load conditions," *IEEE Trans. Ind. Electron.*, Vol. 58, No. 9, pp. 3967-3975, Sep. 2011.

[7] B. Singh and V. Verma, "Selective compensation of power-quality problems through active power filter by current decomposition," *IEEE Trans. Power Del.*, Vol. 23, No. 2, pp. 792-799, Apr. 2008.

[8] S. Rahmani, N. Mendalek, and K. Al-Haddad, "Experimental design of a nonlinear control technique for three-phase shunt active power filter," *IEEE Trans. Ind. Electron.*, Vol. 57, No. 10, pp. 3364-3375, Oct. 2010.

[9] H. Haibing and X. Yan, "Design considerations and fully digital implementation of 400-Hz active power filter for aircraft applications," *IEEE Trans. Ind. Electron.*, Vol. 61, No. 8, pp. 3823-3834, Aug. 2014.

[10] M. Aredes, J. Häfner, and K. Heumann, "Three-phase four-wire shunt active filter control strategies," *IEEE Trans. Power Electron.*, Vol. 12, No. 2, pp. 311-318, Mar. 1997.

[11] F. Z. Peng, G. W. Ott, and D. J. Adams, "Harmonic and reactive power compensation based on the generalized instantaneous reactive power theory for three-phase four-wire systems," *IEEE Trans. Power Electron.*, Vol. 13, No. 5, pp. 1174-1181, Nov. 1998.

[12] G. W. Chang and T.-C. Shee, "A novel reference compensation current strategy for shunt active power filter control," *IEEE Trans. Power Del.*, Vol. 19, No. 4, pp. 1751-1758, Oct. 2004.

[13] H. Li, F. Zhuo, Z. Wang, W. Lei, and L. Wu, "A novel time-domain current-detection algorithm for shunt active power filters," *IEEE Trans. Power Syst*., Vol. 20, No. 2, pp. 644-651, May 2005.

[14] R. S. Herrera and P. Salmeron, "Instantaneous reactive power theory: A reference in the nonlinear loads compensation," *IEEE Trans. Ind. Electron*., Vol. 56, No. 6, pp. 2015-2022, Jun. 2009.

[15] R. S. Herrera, P. Salmeron, and K. Hyosung, "Instantaneous reactive power theory applied to active power filter compensation: Different approaches, assessment, and experimental results," *IEEE Trans. Ind. Electron*., Vol. 55, No. 1, pp. 184-196, Jan. 2008.

[16] S. Buso, L. Malesani, and P. Mattavelli, "Comparison of current control techniques for active filter applications," *IEEE Trans. Ind. Electron*., Vol. 45, No. 5, pp. 722-729, Oct. 1998.

[17] K. M. Smedley, L. Zhou, and C. Qiao, "Unified constant-frequency integration control of active power filters-steady-state and dynamics," *IEEE Trans. Power Electron.*, Vol. 16, No. 3, pp. 428-436, May 2001.

[18] C. Qiao and K. M. Smedley, "Three-phase bipolar mode active power filters," *IEEE Trans. Ind. Appl.*, Vol. 38, No. 1, pp. 149-158, Jan./Feb. 2002.

[19] C. Qiao, J. Taotao, and K. M. Smedley, "One-cycle control of three-phase active power filter with vector operation," *IEEE Trans. Ind. Electron*., Vol. 51, No. 2, pp. 455-463, Apr. 2004.

[20] S. Hirve, K. Chatterjee, B. G. Fernandes, M. Imayavaramban, and S. Dwari, "PLL-less active power filter based on one-cycle control for compensating unbalanced loads in three-phase four-wire system," *IEEE Trans. Power Del*., Vol. 22, No. 4, pp. 2457-2465, Oct. 2007.

[21] K. Chatterjee, D. V. Ghodke, A. Chandra, and K. Al-Haddad, "Modified one-cycle controlled load compensator," *IET Power Electron.*, Vol. 4, No. 4, pp. 481-490, Apr. 2011.

[22] E. S. Sreeraj, E. K. Prejith, K. Chatterjee, and S. Bandyopadhyay, "An active harmonic filter based on one-cycle control," *IEEE Trans. Ind. Electron*., Vol. 61, No. 8, pp. 3799-3809, Aug. 2014.

[23] J. Taotao and K. M. Smedley, "Operation of one-cycle controlled three phase active power filter with unbalanced source and load," *IEEE Trans. Power Electron*., Vol. 21, No. 5, pp. 1403-1412, Sep. 2006.

[24] A. S. Lock, E. R. C. da Silva, D. A. Fernandes and M. Elbuluk, "An OCC-APF control strategy for unbalanced grid conditions," in *Proc. IEEE Appl. Power Electron. Conf.*, pp. 1677-1684, 2015.

[25] X. Yuan, W. Merk, H. Stemmler, and J. Allmeling, "Stationary-frame generalized integrators for current control of active power filters with zero steady-state error for current harmonics of concern under unbalanced and distorted operating conditions," *IEEE Trans. Ind. Appl.*, Vol. 38, No. 2, pp. 523-532, Mar./Apr. 2002.

Lei Wang was born in China, in 1985. He received his M.S. degree from the Taiyuan University of Technology, Taiyuan, China, in 2010, where he is presently working towards his Ph.D. degree in the College of Electrical and Power Engineering. His current research interests include power electronic converters, active and hybrid filters, the application of power electronics in renewable energy systems, and power quality compensation systems.

Chunguang Ren was born in China, in 1989. He received his B.S. degree from the Taiyuan University of Science and Technology, Taiyuan, China, in 2012. He is presently working towards his Ph.D. degree in Taiyuan University of Technology. His current interests include the power electronics interfaces for renewable sources in microgrids and the stability of power converters.

Yu Yang was born in China, in 1975. He received his Ph.D. degree from Xian Jiaotong University, Xi'an, China, in 2007. He is presently working as a Senior Engineer at the Shanxi Electric Power Corporation, Taiyuan, China. His current research interests include power electronics and control, power quality compensation systems, and nonlinear phenomena in power electronic circuits and systems.

Xiaoqing Han received her B.S., M.S., and Ph.D. degrees from the College of Electrical and Power Engineering, Taiyuan University of Technology, Taiyuan, China. She is presently working as a Professor in the Taiyuan University of Technology. Her current research interests include power system simulation, stability analysis, and the integration of renewable energy sources. Professor Han was a recipient of the Science and Technology Award of Shanxi Province, in 2001 and 2005.

Peng Wang received his B.S. degree from Xian Jiaotong University, Xi'an, China, in 1978; his M.S. degree from the Taiyuan University of Technology, Taiyuan, China, in 1987; and his M.S. and Ph.D. degrees from the University of Saskatchewan, Saskatoon, SK, Canada, in 1995 and 1998, respectively. He is presently working as a Professor at the Nanyang Technological University, Jurong West, Singapore.